Contents list available at CBIORE journal website

International Journal of Renewable Energy Development

Journal homepage: https://ijred.cbiore.id

Research Article

Performance of a direct-expansion solar-assisted heat pump for domestic hot water production in Algeria

Sofiane Benchamma[1*], Mohammed Missoum[2], Nefissa Belkacem[1]

[1]*Laboratory of Control, Tests, Measures and Mechanical Simulations, Faculty of Technology, Hassiba Benbouali University of Chlef, Hay Salem, National Road N 19 -02000, Chlef, Algeria.*

[2]*University Centre of Tipaza, Road of Oued Merzoug, 42000, Tipaza, Algeria.*

Abstract. The focus of this study is to investigate the energy performance of a direct-expansion solar-assisted heat pump water heating system (DX-SAHPWH). The system consists of an unglazed solar collector-evaporator, which can absorb heat from solar energy and air ambient simultaneously, a condenser in the form of a coil immersed in a hot water storage tank, a thermostatic expansion valve and a hermetic reciprocating compressor. The performance of the heat pump system is evaluated using a developed mathematical model under Matlab code. The modelling method is based on lumped and distributed parameter approach of different system components. Numerical calculations were carried-out to study the influence of different parameters, such as ambient temperature, solar radiation intensity and polytropic index on the system performance. Additionally, in order to evaluate the long-term system performance, the system's model was applied on a case study of a single-family building located in Djelfa (Algeria), which represents the coldest arid region of the country. The results showed that the solar radiation intensity and ambient temperature have significant effects on the heat pump performance. A COP of 5.9 and a collector-evaporator efficiency of 1.9 were obtained at high solar radiation of 850 W/m^2 resulting in lower heating time (29 min). In addition, results revealed that the system can operate even at lower ambient temperature due to its ability to take advantage of heat from the ambient air. The results from the case study gave a COP ranging from 2.3 to 3.8, which enhance the promising adoption of this system in domestic hot water production to respond to people daily life needs with clean, abundant and renewable energy.

Keywords: Solar thermal energy**;** direct-expansion solar-assisted heat pump**;** hot water production; mathematical modelling; coefficient of performance.

Received: 11th Feb 2024; Revised: 7th April 2024; Accepted: 17th April 2024; Available online: 28th April 2024

1. Introduction

Energy plays an essential role in the functioning of our modern societies, supporting all human activities. The building residential sector consumes 40% of total energy end-use, generating 36% of greenhouse gas emissions (European Commission, 2019). The continued dependence on fossil energy resources presents considerable challenges in terms of environmental impact and sustainability. On the other hand, the increase in energy prices and the decrease in purchasing power on the global scale and on local scale make people struggle to meet the demands of their daily lives and pay their energy bills. This makes the search for abundant and cheap sources a crucial mission of scientists. Faced with these challenges, many countries are turning to renewable energy sources to meet their energy needs, while reducing greenhouse gas emissions and preserving natural resources. In Algeria case, a promising renewable energy program has been launched to increase the renewable energy share in the country energy production (MEM, 2011). The national energy mix program is to attain the objective of 65% solar renewable energy by 2050 (Hasni *et al.*, 2021). Among the renewable energy sources, the use of solar energy has grown significantly in recent decades, covering various fields, including the production of hot water for domestic use. This production is done by technical energy systems such as heat pumps.

A conventional air-source heat pump is a practical installation with low initial investment. It is widely used for domestic hot water production and heating buildings (Leonzio *et al.*,2022). However, its performance is greatly affected by the outdoor ambient temperature, leading to high electrical energy consumption and reduced energy performance particularly in cold climates (Liu *et al.*,2017). Faced with these problems, solar-assisted heat pump (SAHP) emerges as a promising solution that combines the advantages of the conventional heat pump with the use of solar energy to improve its efficiency and reduce its dependence on electricity (Shia *et al.*,2019). A SAHP can be classified into direct and direct expansion systems. In indirect-expansion (IX-SAHP) system, solar collector and the evaporator of heat pump are separated by a heat exchanger. Whereas in direct-expansion system (DX-SAHP) the solar collector plays the role of evaporator, where the refrigerant fluid is evaporated directly by absorbing heat from solar energy (Missoum and Loukarfi, 2021). The production of hot water can be achieved by direct solar heating system, which avoid the electrical consumption of the heat pump compressor (Kaci *et al.*, 2023).

* Corresponding author
Email: s.benchamma@univ-chlef.dz (S. Benchamma)

https://doi.org/10.61435/ijred.2024.60112
ISSN: 2252-4940/© 2024.The Author(s). Published by CBIORE

However, the nature solar radiation fluctuation significantly affects the spreading of such systems.

Glazed flat-plat solar collector is usually used as evaporator in DX-SAHP system. In order to increase solar heat collection and improve consequently the system performance, glazed collector type is replaced by an unglazed one (Sezen and Gungor, 2023). In such system, the heat necessary to evaporate the refrigerant fluid is collected from solar energy in high solar radiation availability. In case of low or absence solar radiation, heat is absorbed from ambient air (Cao, 2020 and Xian, 2020). Indeed, Tagliafico et al., (2014) compared the thermodynamic performance of a DX-SAHP system with three solar collector configurations to satisfy domestic hot water requirements. The annual primary energy savings achieved by the system were 49.5%, 48.5% and 48% for unglazed, glazed and double-glazed panels, respectively. The unglazed collector, the cheapest one, was the good choice for the DX-SAHP.

The meteorological conditions such as solar radiation and ambient temperature have a great influence on the system performance. Kong *et al.,* (2011) investigated by experiment and simulation a DX-SAHP system for domestic hot water. The system uses a bare flat-plate collector as evaporator and R-22 as working fluid. The best daily COP is 6.12 at solar radiation of 955 W/m^2 and ambient temperature of 20.6°C. In another work, Kong *et al.,* (2017) uses R410A as refrigerant fluid instead of R-22. The results showed that when the solar radiation increases from 300 to 900W/m^2, the COP rises from 4.1 to 6.0. Whereas, the thermal efficiency and heating time decrease from 2.1 to 1 and 85 min to 64 min, respectively.

The collector-evaporator type and structure have also significant effect on the performance of the heat pump. Sun *et al.*, (2014) investigated a system with a roll-bond solar collector-evaporator using three different channel patterns (parallel shape, fractal T-shape and honeycomb shape) under the same cross section area. The hexagon shaped channel was the optimal geometric structure, which results in an increase of COP of 5.9% and heating capacity of 6.2%, compared to T-shape panel. The COP of around 5.5 and the thermal efficiency of around 1.25 at a solar radiation and ambient temperature of 700 W/m^{2}and 26 °C were obtained. Ji *et al.*, (2020) performed an experimental study of a DX-SAHP with a finned tube evaporator. The COP of the system increases from 2.24 to 2.41 with solar radiation varying from zero to 400W/m^2. While the COP was 2.22, 2.42 and 2.58 when the ambient temperature was 5, 10 and 15°C. Moreover, the finned tube evaporator was compared to a bare plate one. It was found that the COP increases by 6.6 % and 16.2 % for bare plate and finned tube, respectively, with the rise of ambient temperature from 5 to 15°C. Cai *et al.*, (2019) studied a system with finned tube evaporator and collector evaporator connected in series. An average COP of 2.71 was obtained at the solar irradiation of 100 W/m2 and ambient temperature of 10°C. Furthermore, diverse types of solar collector-evaporator have been used. For example, air-cooled heat exchanger (Fu *et al.*, 2012), tube-in-sheet (Huang *et al.* 2001), finned-tubes (Cai *et al.*, 2017 and Deng *et al.*, 2016), forced-air heat exchanger (Kuang *et al.*, 2006), micro-channel (Wu *et al.*, 2019), flat-plate evaporator with straight fin (li *et al.*, 2018), air finned coil heat exchanger (Zanetti*etal.*, 2023).

The impact of structural parameters and refrigerant charge and type have been also considered in number of studies. Kong *et al.*, (2022) studied the influence of refrigerant charge and condenser area on the thermal performance of a heat pump system with a micro-channel collector/evaporator. The results showed that as the condenser area increased from 0.553 to 1.393 m^2, the maximum COP and corresponding optimal refrigerant charge increased by 8.95 % and 27.91 %, respectively. Chata *et al.*, (2005) investigated the effect of several refrigerants using two collector configurations, namely a bare collector and a one cover collector. Results showed that R-12 produces the highest value of COP, followed by R-22 and R-134A. For the mixture refrigerants, R-410A was shown to be more efficient than either R-407C or R-404A but not as good as R-134A. The refrigerant R-410A produced COP values that are 15-20 % lower than those obtained with R-134A. Duarte *et al.*, (2019) compared between some refrigerants in terms of thermal performance and environmental impact, R134a is the reference and low global warming refrigerants are R290, R600a, R744 and R1234yf. The results showed that R290 has a better COP for solar irradiance between 300 W/m^2 and 700 W/m^2 and an ambient temperature between 10°C and 35°C, while for a solar irradiance less than 50 W/m^2, R134a has a better COP than R290. Zhang *et al.*, (2014) studied the performance of the system by varying the refrigerant charge, solar collector area, collector thickness, condenser pipe length and diameter. The results indicated that a refrigerant charge between 1.65-1.75kg, collector area 6m^2, condenser pipe length 70m and condenser internal diameter 9mm lead to better performance of a HP. Kong *et al.*, (2020) made a quasi-dynamic model of a DX-SAHP for water heating in order to know the influence of different compressor speed regulation modes on the system performance. The results showed that with a compressor speed of 2900 rpm, the COP exceeds 4.6, while when the compressor speed decreases from 2910 to 2650 rpm the COP increases by 7.5%.

The major of the above-mentioned works on DX-SAHPWHs have not considered seasonal conditions effect on the system performance. In this trend, the main objective of this study is to contribute in the evaluation of the performance of a direct-expansion solar assisted heat pump water heating on daily, monthly and yearly basis. First, a parametric study is carried-out to investigate the influence of solar radiation, ambient temperature and polytropic index on the system performance. Then, in order to evaluate long-term system performance, a case study of single-family building located in a cold region of Algeria was performed.

2. Methodology

2.1 Description of the system

The studied DX-SAHP system comprises four essential elements: a flat-plate unglazed collector-evaporator, a condenser in the form of a coil immersed in storage tank (ST) for hot water (HW), a thermostatic expansion valve (EV) and a hermetic reciprocating compressor, see Figure1. R134a is used as refrigerant, which is considered among the most efficient fluids in energetic as well as environmental from points of view. The refrigerant circulates in a closed circuit by passing through different system components and undergoes phase change processes. Exiting the expansion valve at low temperature and low pressure, the refrigerant fluid enters into the collector-evaporator and absorbs heat gained from solar radiation/or ambient air where it becomes a superheated vapor. In the compressor, it becomes a vapor at high temperature and high pressure. In the condenser, the refrigerant vapor releases heat to be a saturated liquid. At the level of the expansion valve, the pressure of the liquid refrigerant is reduced. Finally, the cycle is repeated as the refrigerant enters the evaporator-collector. The studied system is equipped with a control subsystem, which has the role of regulating the quantity of refrigerant at the outlet of the collector-evaporator by adjusting the refrigerant flow rate at the level of the expansion valve. When the temperature of the refrigerant at the collector outlet is higher than the considered

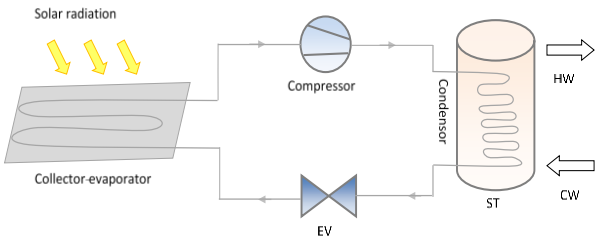

Fig 1. Schematic illustration of a DX-SAHP system

superheat temperature, the refrigerant flow is increased to recover the superheat. In contrast, the flow rate is decreased allowing the refrigerant to become superheated vapor. This configuration protects the compressor against corrosion by avoiding the presence of liquid.

2.2 Presentation of the case study

As mentioned above, the objective of the work is to contribute in the improvement of people daily life in Algeria by reducing the rising energy cost through the exploitation of the abundant and free solar energy (Bouraiou *et al.*, 2019). To obtain better performance and higher energy efficiency, it is suitable to install the heat pump intended for the production of DHW in a region of Algeria where temperatures in winter drop to the lowest degrees. Highland regions of Algeria are characterized by cold winters. Among them, the city of Djelfa is considered as the case study. Djelfa city is located at 34.67° N and 3.25° E with 1080 m of Altitude.

The system performances are calculated based on a daily hot water consumption of 240 litters per day at 50°C (Baki *et al.*, 2022). The hot water is used for different household needs, such as showering, cooking, washing machine and dishwasher. The monthly mean cold water temperatures from the main network are presented in Table 1. (Meteonorm 8, 2022).

The tilt angle of the collector-evaporator is (β=35°) to collect maximum solar radiation and it is oriented southward (γ=0). The tilt angle is chosen according to the latitude of the site (Darhmaoui *et al.*, 2013). Figure 2 illustrates the daily variation of temperatures in the city of Djelfa (Meteonorm 8, 2022). During summer months, temperatures are the highest, with a peak in July averaging 38°C, while they drop significantly during the winter months with an average of -5°C in January and February. This significant drop in winter temperatures has an impact on the need for daily-life domestic water heating. The city of Djelfa, being faced very low ambient temperatures in winter, therefore requires attention in terms of DHW needs.

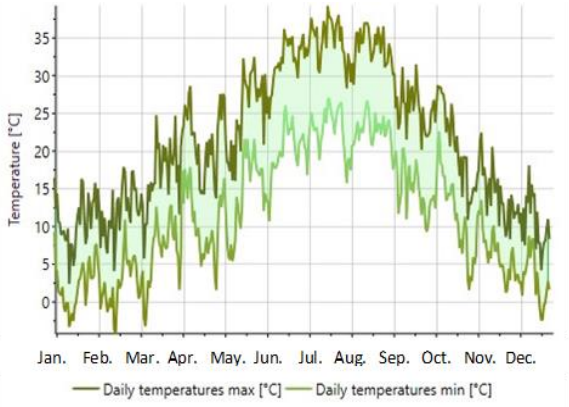

Fig. 2. Monthly variation of temperature in Djelfa

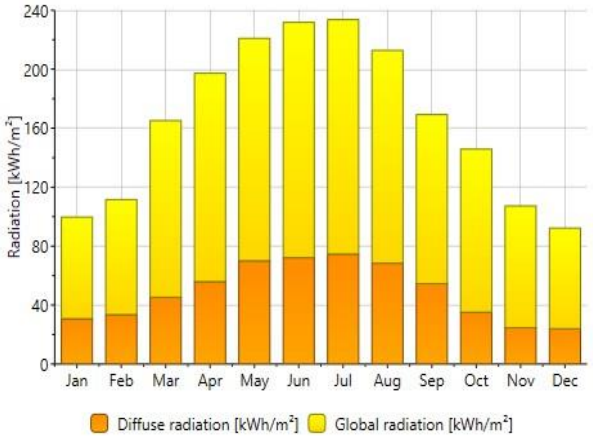

Fig.3. Monthly variation of solar radiation in Djelfa

Table1
Data of network cold water and ambient temperature

Months	T_{CW} (°C)	T_a (°C)
Jan	6,9	5,9
Feb	8	7
Mar	9,9	10,9
Apr	13,7	14,7
May	18,4	19,4
Jun	24,3	25,3
Jul	28,4	29,4
Aug	27,1	28,1
Sep	21,6	22,6
Oct	18,6	17,6
Nov	11,4	10,4
Dec	7,9	6,9

Furthermore, a correlation is observed between solar radiation and ambient temperature, which indicates that there is a proportional relationship between solar radiation received in the region and ambient temperature. Thus, the higher the solar radiation, the more the ambient temperature increases.

Figure 3 highlights the monthly variation of solar radiation in the city of Djelfa. In summer months, irradiance reaches higher levels with a peak in July of 225 kWh/m^2 whereas in winter months it is at a lowest level with a record of 87.5 Wh/m^2 in December. It is again worth noticing the need to introduce a DX-SAHP system to comply heating needs in this region.

2.3 Mathematical modeling

The mathematical models of the different system components are developed by taking into account some assumptions: thermal and physical properties are used at steady-state conditions; the small pressure losses in the collector-evaporator and pipes are ignored and the refrigerant vapor at the collector-evaporator outlet is considered as a saturated vapor. Based on the above assumptions, a simple mathematical model is developed to describe the system performance. The thermodynamic properties of R134a refrigerant for different system components corresponding to various refrigerant phases are taken from REFPROP7 (Lemmon *et al.*, 2013).

2.3.1 Collector-evaporator model

A bare flat plate solar collector without back insulation is used in the DX-SAHP system, which is able to absorb heat from both solar energy and air ambient. The saturated liquid refrigerant entering the collector-evaporator passes to a liquid-vapor phase

inside. At the outlet of the collector-evaporator, a superheat degree of 10°C is considered. The useful heat gain of solar collector/evaporator (Q_{coll}) is evaluated as follows:(Duffie *et al.*, 2013 and Kong *et al.*, 2017).

$$\boldsymbol{Q_{coll} = A_c F'[S - U_L(T_{rm} - T_a)]} \quad (1)$$

Where A_c is the solar collector-evaporator area, F' is the collector efficiency factor, T_{rm} is the average temperature of the refrigerant at the solar collector-evaporator and T_a is the ambient temperature.
The efficiency factor F' is given by (Ito *et al.*, 1999):

$$F' = F + (1 - F)\left(\frac{d}{w}\right) \quad (2)$$

Here w is the distance between the pipes, d is the external diameter of the pipe and F is the efficiency of fins, which is evaluated as:

$$F = \frac{\tanh(U_b)}{U_b} \quad (3)$$

Where U_b is a dimensionless number given by:

$$U_b = \frac{w-d}{2}\sqrt{\frac{U_L}{k.\delta}} \quad (4)$$

k and δ are the thermal conductivity and the thickness of the collector plate respectively.
The symbol S is calculated as:

$$S = \theta I - \varepsilon q_0 \quad (5)$$

Where θ is the absorptivity of the collector plate, I is the solar radiation intensity on the collector plate, ε is the emissivity of the collector plate, and q_0 is the difference between the emissive power per unit area from a black body at the ambient air temperature and the emissive power from the sky, as given:

$$q_0 = \xi T_a^4 - q_\infty \quad (6)$$

Where ξ is the Stefan–Boltzmann constant with the value of 5.67 × 10−8 W m^{-2} K^{-4}, and q_∞ is the sky radiation.
The symbol U_L can be expressed by:

$$U_L = \alpha + 4\varepsilon\xi T_a^3 \quad (7)$$

Where α is the convective heat transfer coefficient.
The refrigerant heat gain at the solar collector level is given by:

$$Q_r = \dot{m}_r.\left(h_{out,SCE} - h_{in,SCE}\right) \quad (8)$$

The mean refrigerant temperature can be drawn from the equality of the solar collector heat gain and the heat gained by the refrigerant fluid (Q_r) expressed as:

$$Q_{coll} = A_c F'[S - U_L(T_{rm} - T_a)] = \dot{m}_r.\left(h_{out,SCE} - h_{in,SCE}\right) \quad (9)$$

Where $\dot{m}_r$ is the refrigerant mass flow rate, $h_{out,SCE}$ is the outlet enthalpy of solar collector evaporator and $h_{in,SCE}$ is the inlet enthalpy of solar collector evaporator.

2.3.2 Compressor model

For a small-scaled rotary-type and hermetic compressor, the refrigerant mass flow rate ($\dot{m}_r$) is given as (Kong *et al.*, 2022):

$$\dot{m}_r = \frac{N.\varphi.V_d}{60.v_{suc}} \quad (10)$$

Where N is the compressor rotational speed, v_{suc} is the specific volume of the refrigerant at the inlet of the compressor, φ is the volumetric efficiency of the compressor, and V_d is the displacement volume rate of the compressor. Neglecting the pressure drop at the inlet and outlet of the compressor, the electrical power consumption of the compressor can be determined as follows (Wu, 2004):

$$W_{com} = m_r \frac{P_{suc}.v_{suc}}{\eta_{com}}.\frac{k}{k-1}\left[\left(\frac{P_{dis}}{P_{suc}}\right)^{\frac{k-1}{k}} - 1\right] \quad (11)$$

Where P_{suc} and P_{dis} are the suction pressure and discharge pressure of the compressor [bar], η_{com} is the total efficiency of the compressor, and κ is the polytropic index of the refrigerant fluid.

2.3.2 Condenser model

Assuming uniform tank temperature and perfect heat transfer between the refrigerant and water, the heat released by the refrigerant across the condenser is equivalent to that absorbed by water that say:

$$Q_{cond} = Q_w \quad (12)$$

The heat gain in the condenser Q_w can be calculated as follows (Sun *et al.*, 2015):

$$Q_w = M_w.C_w.\frac{dT_w}{dt} \quad (13)$$

Where M_w is the total mass of the water in water tank, C_w is the specific heat of water, T_w is the water temperature, and t is the heating time.

$$Q_{cond} = \dot{m}_r.\left(h_{in,cond} - h_{out,cond}\right) = M_w.C_w.\frac{dT_w}{dt} \quad (14)$$

Where $h_{out,cond}$ is the enthalpy at the outletof the condenser and $h_{in,cond}$ is the enthalpy at the inlet of the condenser.
Therefore, water temperature with respect-to-time was calculated using the following formula:

$$T_w = \frac{\dot{m}_r}{M_w.C_w}\left(h_{in,cond} - h_{out,cond}\right).t + T_{w,initial} \quad (15)$$

Where $T_{w,initial}$ is the initial water temperature.

The equations are solved by a numerical iteration method using the developed MATLAB program taking into account the interactions between the various models of system components. The flow-chart in figure 4 describes the sequence of calculations. After reading the program inputs such as metrological and structural parameters, evaporation and condensation pressures were assumed. Then, the compressor work and the mass flow rate as well as the solar collector evaporator heat gain and the mean refrigerant temperature are calculated. Subsequently, the temperatures of the refrigerant (T_{rm}) and evaporating temperature (T_{evap}) are compared. If the absolute value between them is greater than the superheat degree (ΔT), the evaporating pressure is adjusted. Otherwise, the calculation procedure continues by calculating the condenser heat gain and the tank water temperature. If the latter is lower than the set-point temperature, the time-step is incremented until the required temperature is reached.

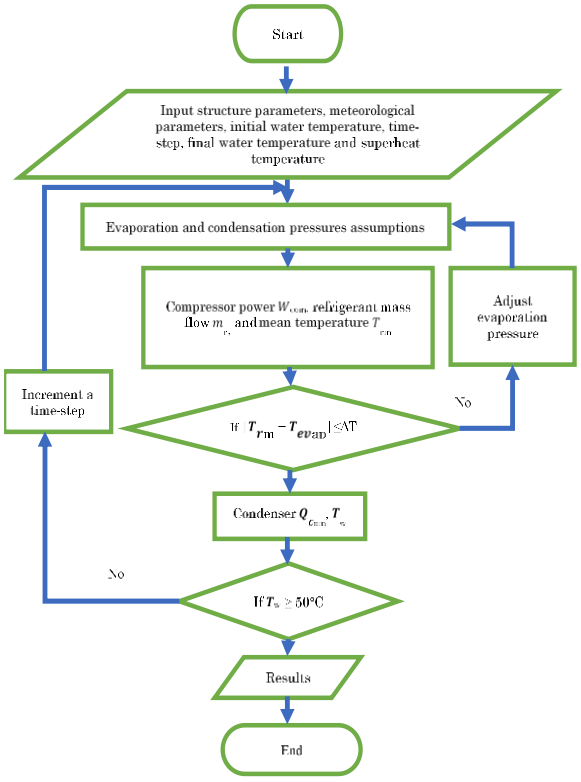

Fig. 4. Solution algorithm for predicting DX-SAHP system performance

3. Simulation results and discussions

In this section, the energy performance of the considered DX-SAHP system is presented and discussed starting by a parametric study and followed by a case study. The parametric study aims to evaluate the influence of solar radiation and ambient temperature on the system performance. Whereas in the case study, the long-term performance of the solar system for DHW supply of a typical single-family building in Algeria is studied.

3.1 Parametric study

3.1.1 Influence of solar radiation

To study the influence of solar irradiance on the system performance, a constant ambient temperature (20°C) and variable intensity of solar irradiance from 100-1000 W/m² are considered. Figure 5 shows the variations of collector-evaporator efficiency and COP with the solar irradiation. It can be seen from figure 05 that the efficiency decreases sharply from 100 to 200 W/m² and gradually between 200 and 600 W/m². After that, the effect of solar irradiation on thermal efficiency is not noticeable. The maximum value of thermal efficiency is 1.9 at low irradiance (100 W/m²). This is because the collector-evaporator collects both solar energy and air thermal energy in one hand. In other hand, as the collector temperature is lower than the ambient temperature, this deduces more heat collection capacity, thus better efficiency. This discussion is in line with revealed results reviewed by (Sezen and Gungor, 2023) showing that DX-SAHP are preferred under 400 W/m² irradiances.

However, when the irradiation increases, the collector begins to superheat and its temperature becomes higher than the ambient temperature. Therefore, it can no longer capture

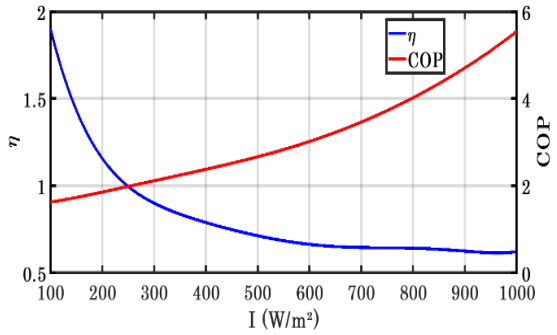

Fig. 5. Variation of COP and solar collector efficiency as a function of solar radiation intensity

energy from the surrounding air and is limited to solar energy. This explains the decrease in efficiency with the increase in solar irradiance. This suggests that low intensity sunlight, combined with atmospheric energy, results in a better energy efficiency. On the other hand, when the solar irradiation increases, the efficiency decreases due to superheating of the collector and due to its main dependence on solar energy rather than on the energy of the ambient air. This observation highlights the importance of designing collector-evaporator systems that can effectively regulate temperature and maximize the use of ambient energy while minimizing the adverse effects of superheating.

The increase in solar irradiation has a positive impact on the COP. Indeed, when solar irradiation increases, the refrigerant absorbs more heat, which increases the vapor temperature at the compressor inlet and makes it possible to reduce the electrical consumption. Consequently, it reduces the dependency on polluting fossil energy sources. As a result, more heat is transferred to the water through the condenser; higher values of COP are obtained. When solar radiation increases from 100 to 1000 W/m², the COP rises from 1.62 to 5.55, which agree with previous works. For example, in an earlier study performed on DX-SAHPWH by Coa *et al.*, (2020), the predicted and experimental COPs obtained at 1000 W/m² were 5.6 and 5.8, respectively.

Figure 6 illustrates the influence of solar irradiance on the heating time for different water volume from 100 to 500 liters of water up to 50°C. For all water volumes, it is clear that the heating time is inversely proportional to solar irradiance. With limited solar irradiance, the amount of solar energy captured by the refrigerant is also reduced, which extends time required to reach the desired water temperature in the storage tank. On the other hand, when the solar irradiation is high, the heating time of the water is reduced to the half due to the fact that with abundant solar radiation, the collector captures more solar energy hence it heats the water faster. Secondly, it is observed that the water quantity has an important effect on the heating time with the same behavior for all different volumes. Indeed, the heating time increases with the rise of water volume. For example, the heating time is more than doubled when the volume changes from 100 to 500 liters.

The curves of figure 7 represent the variation of heating time as a function of water temperature in the storage tank with three levels of solar radiation: low, medium and high. The three solar radiation intensities of 250, 450 and 850 W/m2 correspond to winter, mi-season and summer, respectively. Obviously, with the three different levels of solar irradiances, the desired water temperature was reached at different heating times. The higher the solar irradiance, the lower heating time is. With low irradiation (250 W/m²), the quantity of solar energy

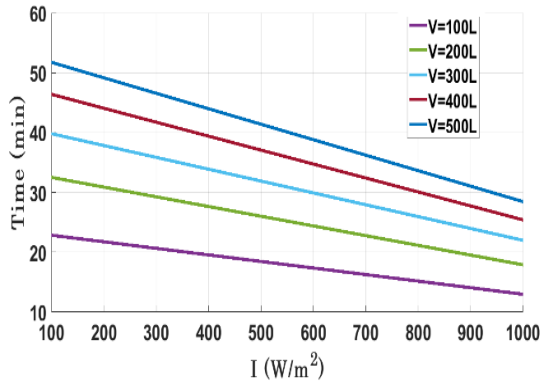

Fig.6. Variation of heating time with solar radiation

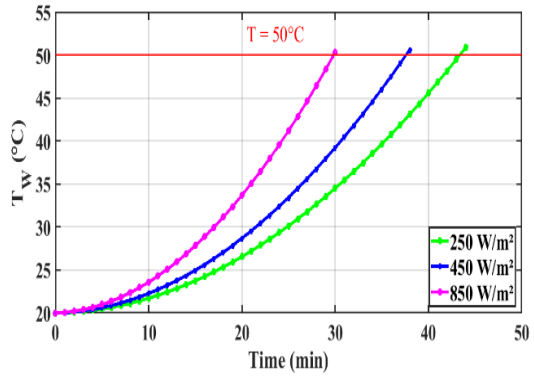

Fig.7. Influence of heating time on water temperature at three different solar irradiations

captured is insufficient to heat the water quickly (40 minutes). At medium irradiance (450 W/m^2), the heating time is reduced to (36minutes). During high solar irradiance (850 W/m^2), the heating time is considerably reduced to more than one-quarter time (29 minutes). It can be concluded that the heating time is inversely proportional to the solar irradiance.

3.1.2 Influence of ambient temperature

The influence of ambient temperature is studied for a constant solar irradiance of (250 W/m^2), to assess the performance of the system under the most adverse conditions, and for a range of ambient temperature between 5-35°C. Figure 8 depicts the variations of the collector-evaporator efficiency and the COP. It is well observed that the efficiency and the COP increase as the ambient temperature increases (Coa *et al.*, 2020). For example, at an ambient temperature of 0°C, the efficiency is 0.6 with a

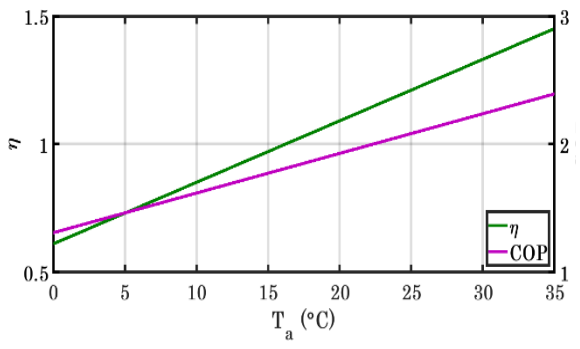

Fig. 8. Influence of ambient temperature on system performance

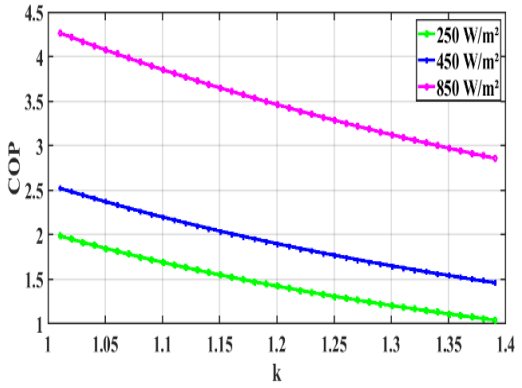

Fig. 9. Variation of COP as a function of polytropic index

COP of 1.7; which indicates that even with overcast sky and a very low ambient temperature, the system can operate. In addition, as the ambient temperature rises, the system exhibits better performance, which means that the system can operate with ambient air energy alone, even in the absence of irradiance. It is also noted that at the low radiation the increase in the collector-evaporator efficiency with the increase in ambient temperature is because of the collector mainly absorbs atmospheric energy, while the solar energy contribution is almost negligible, which avoids any superheating of the collector-evaporator.

3.1.3 Influence of the polytropic index

The curves of figure 9 represent the variation of COP as a function of polytropic index (k) for the different solar radiations. Two polytropic indexes 1 and 1.4, which correspond to isothermal compression and reversible and adiabatic compression are considered (Okawa *et al.*, 2021). As expected, in summer the system shows higher performance (COP=4.6) followed by the midseason period (COP=2.9) and then in winter (COP=2.4); which is justified by the decreasing solar radiation between these times of the year. In the three cases of irradiances, it can be observed that the COP decreases with the increase in the polytropic index. In isothermal compression, where (k=1), the temperature of the refrigerant remains constant because of an optimal heat transfer with the surroundings, which keeps the enthalpy of the fluid constant. As a result, the amount of heat transferred to water during condensation remains constant, resulting in a minimal COP. On the other hand, in isentropic compression (reversible and adiabatic), where k=1.4, the temperature of the refrigerant further increases the fact that there is no heat transfer with the outside and no energy loss. This means that the enthalpy of the fluid here is greater than that of the polytropic case. As a result, the amount of heat transferred to the water will increase, resulting in a decrease in COP.

3.1.4 Influence refrigerant evaporating pressure on refrigerant mass flow rate

Figure 10 shows the effect of refrigerant evaporating pressure on refrigerant mass flow rate. A proportional relationship between evaporating pressure and refrigerant mass flow rate is noticed. The higher the refrigerant evaporating pressure, the higher the refrigerant mass flow rate. Because of the increase of refrigerant evaporating pressure caused by its temperature elevation due to solar heat absorption, the difference between the evaporation temperature and ambient temperature is

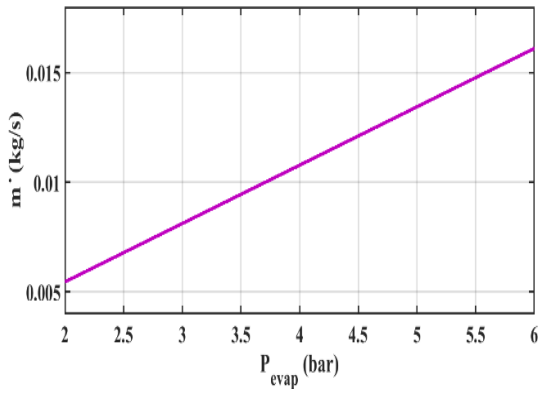

Fig. 10. Influence of refrigerant evaporation pressure on refrigerant mass flow

reduced. Therefore, the required heat leading to a superheated vapor is decreased. In other words, when the set superheated degree (10°C) is reached, the refrigerant mass flow rate increases to allow the exceeding absorbed solar heat to be transferred to the HP condenser, which in turn augments the DHW production.

3.2 Case study results

Figure 11 illustrates the thermal energy collected by the solar-collector evaporator and that supplied by the heat pump condenser. During summer months, there is a significant increase in the amount of heat absorbed by the collector-evaporator and consequently an increase in the amount of heat transferred to water by the condenser. This is due to the intense sunlight and high ambient temperatures during this period. It is also noticeable that during the colder months such as January, the system absorbs thermal energy of approximately 785.62 kWh and products DHW by approximately 957.65 kWh, which proves that the system can be functional, even under the most adverse conditions of the year. The histogram on Figure 12 represents the monthly variations in the COP and the efficiency of the evaporator collector in Djelfa. It is observed that during summer months, July and August, the COP and the efficiency reach their maximum values 3.8 and 0.8 respectively. This is mainly due to the abundance of solar and atmospheric energy, allowing the system to capture more heat for the heating process. During the winter months as in January, despite the low temperatures and the low irradiance, the system gives an

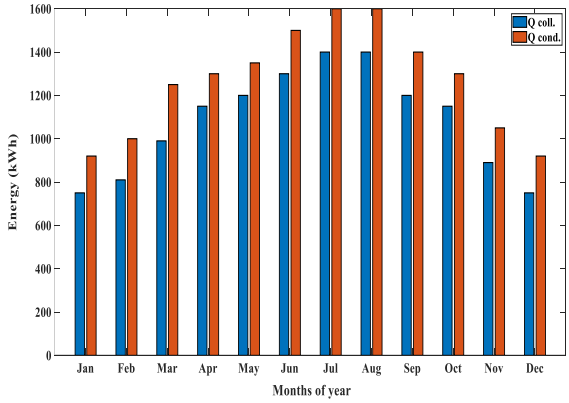

Fig. 11. Monthly variation of heat collected and supplied by the system

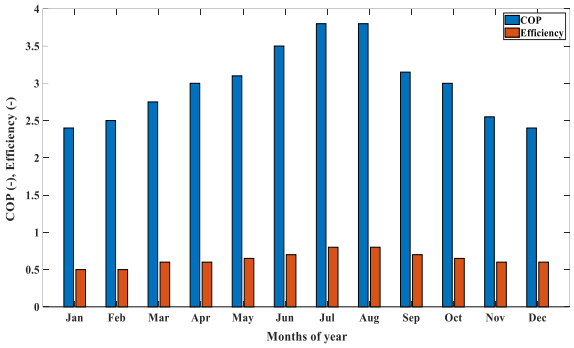

Fig. 12. Monthly variation of heat pump COP and solar collector efficiency.

optimal value of the collector efficiency (η=0.6) which means that it can absorb atmospheric energy since its temperature is lower than the ambient temperature because the boiling temperature of R134a is very low. The (COP=2.3) is very low due to the high compressor power consumption to further increase the fluid temperature in order to satisfy the need for heating. It can be concluded thus, the system is adaptable to the climatic conditions of Djelfa city, with optimal performance during the summer months and acceptable performance during the coldest winter months.

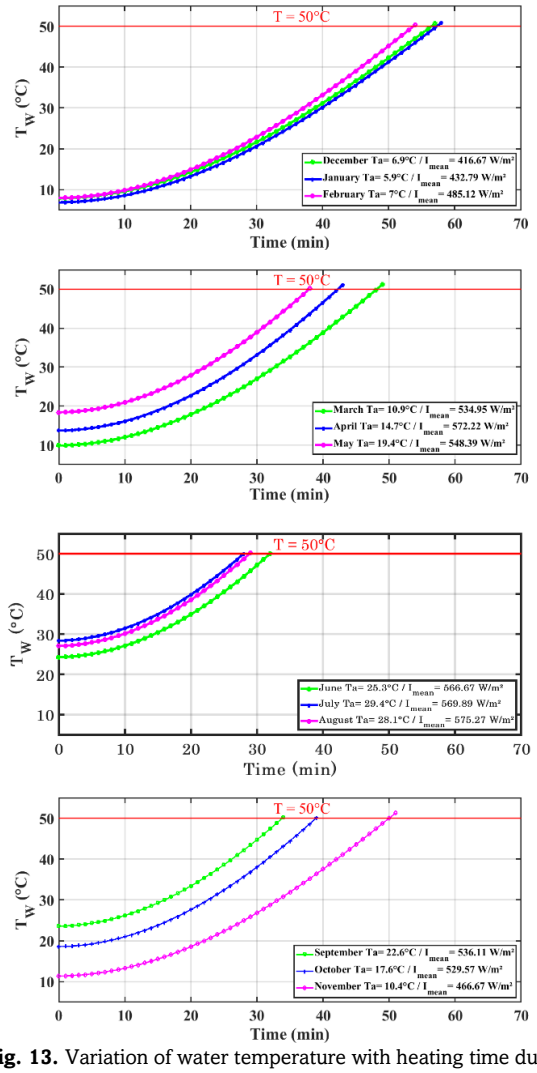

Fig. 13. Variation of water temperature with heating time during seasons (a) -winter, (b) -spring, (c)-summer, (d)-autumn.

The heating time needed to heat water up to 50°C is calculated by considering the average mean ambient temperature and solar energy intensity of each month of the year. Figure 13 represents the variation of water temperature with respect to heating time during the different seasons of the year. It is clear that to reach the desired water temperature of 50°C, the heating time differs from a season to each other. The heating time is directly related to outdoor metrological conditions. The hotter the season, the lower the heating time. The highest value (57.2 min) is obtained in winter (13a) and lowest value in summer (26.5 min), see figure (13c). This can be explained by the strong effect of solar radiation followed by ambient temperature on the evaporating temperature, as proven by Yin, *et al.* (2023) and Deng, *et al.* (2016). The higher evaporating temperature makes the specific volume at the compressor suction inlet decrease, which leads to a high mass flow rate. Therefore, the solar collector heating capacity augments and the heating time decreases.

It can be also noticed that this effect is significant in autumn (13d) following by spring (13b), justified by the gap between lines in the same season. This is because the solar radiation and ambient temperature differences between the months of mi-season are important.

4. Conclusion

In this work, the energy performance of a direct-expansion solar assisted heat pump for hot water production was investigated in a cold climate region of Algeria. The system consists of an unglazed solar collector-evaporator, a coil immersed condenser in a storage tank, a thermostatic expansion valve and a hermetic reciprocating compressor. First, a parametric study was carried out to investigate the effect of meteorological conditions on the system performance. Then, a case study of a residential building was studied.

The parametric study performed demonstrated that the performance of the system is influenced strongly by the solar radiation intensity and ambient temperature. The COP of the heat pump increases as the solar radiation intensity increases. A COP of 5.9 was obtained at high solar radiation of 850 W/m^2 with a collector-evaporator efficiency of 1.9, resulting in lower heating time (29 min). Furthermore, the polytropic index has an inverse effect on the COP regardless the solar intensity. In addition, results revealed that even at lower ambient temperature (0°C), an efficiency of 0.6 and a COP of 1.7 were achieved owing to the ability of the solar collector to absorb heat from the ambient air. This prove that the system can operate under overcast sky and very low ambient temperatures.

The results from the long-term performance of the case-study city revealed that the system can efficiently guarantee DHW supply over the whole year. In summer months, the maximum COP and efficiency are 3.8 and 0.8, respectively. In winter months, the minimum COP is 2.3 and the minimum efficiency is 0.6. The obtained results in this work highlight the promising adoption of this type of facility, which focused on energy savings, clean energy and sustainable development.

Conflicts of Interest: The authors declare no conflict of interest.

References

Baki, T., Sandid, A. M., Nehari, D. (2022) Sizing of an autonomous individual solar water heater based in Oran, Algeria, *Slovak journal of civil engineering*, 30(3), 9 – 16. https://doi.org/10.2478/sjce-2022-0016

Bouraiou, A., Neçaibia, A., Boutasseta, N., Mekhilef, S., Dabou, R., Ziane, A., Sahouane, N., Attoui, I., Mostefaoui, M., Touaba, O., (2019) Status of Renewable Energy Potential and Utilization in Algeria, *Journal of Cleaner Production*, https://doi.org/10.1016/j.jclepro.2019.119011

Cai, J., Ji, J., Wang, Y., Zhou, F., Yu, B. (2017) A novel PV/T-air dual source heat pump water heater system: Dynamic simulation and performance characterization, *Energy Conversion and Management* 148, 635–645. http://dx.doi.org/10.1016/j.enconman.2017.06.03

Cai, J., Li, Z., Ji, J., , Zhou, F. (2019) Performance analysis of a novel air source hybrid solar assisted heat pump. *Renewable Energy* 139, 1133e1145. https://doi.org/10.1016/j.renene.2019.02.134

Cao Y., Mihardjo, L.W.W, Parikhanic, T. (2020) Thermal performance, parametric analysis, and multi-objective optimization of a direct-expansion solar-assisted heat pump water heater using NSGA-IIand decision makings. *Applied Thermal Engineering* 181, 115892. https://doi.org/10.1016/j.applthermaleng.2020.115892

Chata, F. B. G., Chaturvedi, S.K., Almogbel, A.(2005) Analysis of a direct expansion solar assisted heat pump using different refrigerants, *Energy Conversion and Management* 46, 2614–2624. https://doi.org/10.1016/j.enconman.2004.12.001

Darhmaoui, H. and Lahjouji, D. (2013) Latitude Based Model for Tilt Angle Optimization for Solar Collectors in the Mediterranean Region, *Energy Procedia* 42, 426 – 435. https://doi.org/10.1016/j.egypro.2013.11.043

Deng, W., Yu, J. (2016) Simulation analysis on dynamic performance of a combined solar/air dual source heat pump water heater, *Energy Conversion and Management* 120, 378–387, http://dx.doi.org/10.1016/j.enconman.2016.04.102.

Duffie, J. A., William, A., Beckman, A. W. (2013) Solar Engineering of Thermal Processes. 4th Ed. Published by John Wiley & Sons. https://doi.org/10.1002/9781118671603

Duarte, W. M., Paulinoc, T. F., Pabond, J. J. G., Sawalhae, S., Machado, L. (2019) Refrigerants selection for a direct expansion solar assisted heat pump for domestic hot water, *Solar Energy* 184, 527-538. https://doi.org/10.1016/j.solener.2019.04.027

European Commission (2019), going climate-neutral by 2050. P20.

Fu, H. D., Pei, G., Ji, J., Long, H., Zhang, T., Chow, T.T. (2012) Experimental study of a photovoltaic solar-assisted heat-pump/heat-pipe system, *Applied Thermal Engineering* 40, 343e350. https://doi.org/10.1016/j.applthermaleng.2012.02.036

Hasni, T., Malek, R., Zouioueche, N. (2021), l'Algérie 100 % énergies renouvelables, étude ; Friedrich Elbert Stiftung. https://algeria.fes.de

Huang, B. J. and Chyng, J. P. (2001) Performance characteristics of integral type solar-assisted Heat pump, *Solar Energy*. 71(6), 403–414.

Ito, S., Miura, N., Wang, K., (1999) Performance of a heat pumpusing direct expansion solar collectors. *Sol. Energy* 65 (3), 189-196. https://doi.org/10.1016/S0038-092X(98)00124-8

Ji, W., Cai, J., Ji, J., Huang, W. (2020) Experimental study of a direct expansion solar-assisted heat pump (DX-SAHP) with finned-tube evaporator and comparison with conventional DX-SAHP, *Energy & Buildings* 207, 109632. https://doi.org/10.1016/j.enbuild.2019.109632.

Kaci, K., Merzouka, M., Merzouk, N. K., Missoum, M., El Ganaouid, M., Behare, O., Djedjigd, R. (2023) Design, optimization and economic viability of an industrial low temperature hot water production system in Algeria: A case study. *Int. J. Renew. Energy Dev.*, 12 (3), 448-458. https://doi.org/10.14710/ijred.2023.49759.

Kong, X., Zhang, D., Li, Y., Yang, Q. (2011) Thermal performance analysis of a direct expansion solar-assisted heat pump water heater. *Energy*, 36, 6830–6838. https://doi.org/10.1016/j.energy.2011.10.013

Kong, X., Li, Y., Lin, L., Yang, Y. (2017) Modeling evaluation of a direct-expansion solar assisted heat pump water heater using R410A. *Int. J. Refrig.* 76, 136–146. http://dx.doi.org/10.1016/j.ijrefrig.2017.01.020.

Kong, X., Wang, B., Shang, Y., Li, J., Li, Y. (2020) Influence of different regulation modes of compressor speed on the performance of direct-expansion solar-assisted heat pump water heater, *Applied*

Thermal Engineering, Volume 169, 115007. https://doi.org/10.1016/j.applthermaleng.2020.115007

Kong, X., Yan, X., Yue, Z., Zhang, P., Li, Y. (2022) Influence of refrigerant charge and condenser area on direct-expansion solar-assisted heat pump system for radiant floor heating, *Solar Energy,* 247, 499-509.https://doi.org/10.1016/j.solener.2022.10.051.

Kuang, Y. H., Wang, R. Z. (2006) Performance of a multi-functional direct-expansion solar assisted heat pump system, Solar *Energy,* 80, 795–803. https://doi.org/10.1016/j.solener.2005.06.003

Lemmon, E.W., Huber, M.L., McLinden, M.O. (2013) NIST Reference Fluid Thermodynamic and Transport Properties – REFPROP, NIS.

Leonzio, G., Fennell, P. S., Shah, N. (2022) Air-source heat pumps for water heating at a high temperature: State of the art, *sustainable energy technologies and assessments,* 54, 102866. https://doi.org/10.1016/j.seta.2022.102866

Li, H. and Sun, Y. (2018) Operational performance study on a photovoltaic loop heat pipe/solarassisted heat pump water heating system, *Energy and Buildings* 158, 861–872.https://doi.org/10.1016/j.enbuild.2017.10.075

Liu, Z., Wang, Y., Xie, Z., Yu, H., Ma, W.(2017) The related problems and development situation of air source heat pump in the cold and serve cold climate areas, *Procedia Engineering,* 205, 368–372. https://doi.org/10.1016/j.proeng.2017.10.385

MEM (Ministère de l'Energie et des Mines) Programme des Energies Renouvelables et de l'Efficacité Energétique, 2011.

MEM (Ministère de l'énergie et des mines). *Agence Nationale pour la Promotion et Rationalisation de l'Utilisation de l'énergie* (APRUE), Consommation Energétique Finale de l'Algérie, 2017, www.aprue.org.dz

Meteonorm 8. (2022). Meteonorm Software Worldwide Europe irradiation data. Intersolar Europe. https://meteonorm.com/en/news

Missoum, M., Loukarfi, L. (2021) Investigation of a Solar Poly generation System for a Multi-Story Residential Building-Dynamic Simulation and Performance Analysis. *Int. Journal of Renewable Energy Development.* 10(3), 445-458. https://doi.org/10.14710/ijred.2021.34423.

Okawa, T., Asano, H., Ito, K., Mori, S., Umekawa, H., Matsumoto, R., Pyeon, C. H., Ito, D. (2021) Fundamentals for power engineering, *Fundamentals of Thermal and Nuclear Power Generation*, 1, 77-226. https://doi.org/10.1016/B978-0-12-820733-8.00003-0.

Sezen, K., Gungor, A. (2023)Comparison of solar assisted heat pump systems for heating residences: A review, *Solar Energy*, 49, 424-445.https://doi.org/10.1016/j.solener.2022.11.051.

Shia, G. H., Ayeb, L., Lia, D., Duc, X. J.(2019) R.ecent advances in direct expansion solar assisted heat pump systems: A Review, *Renewable and Sustainable Energy Reviews* 109, 349–366.https://doi.org/10.1016/j.rser.2019.04.044

Sun, X., Wu, J., Dai, Y., Wang, R. (2014) Experimental study on roll-bond collector/evaporator with optimized channel used in direct expansion solar assisted heat pump water heating system, *Applied Thermal Engineering* 66, 571-579. http://dx.doi.org/10.1016/j.applthermaleng.2014.02.060.

Sun, X., Dai, Y., Novakovic, V., Wu, J., Wang, R. (2015) Performance comparison of direct expansion solar-assisted heat pump and conventional air source heat pump for domestic hot water; *Energy Procedia* 70, 394 – 401. https://doi.org/10.1016/j.egypro.2015.02.140

Tagliafico, L. A., Scarpa, F., Valsuani, F. (2014) Direct expansion solar assisted heat pumps - A clean steady state approach for overall performance analysis, *Applied Thermal Engineering* 66, 216-226. http://dx.doi.org/10.1016/j.applthermaleng.2014.02.016.

Wu, Y.Z., (2004) Miniature Refrigeration Equipment DesignGuidelines. Machinery Industry Press, Beijing, pp. 66–214.

Wu, J., Xian, T., Liu, X. (2019) All-weather characteristic studies of a direct expansion solar integrated air source heat pump system based on PCMs, *Solar Energy* 191, 34-45. https://doi.org/10.1016/j.solener.2019.08.057

Xian, T., Wu, J., Zhang, X. (2020) Study on the operating characteristics of a solar heat pump water heater based on data fusion. *Solar Energy* 212, 113–124. https://doi.org/10.1016/j.solener.2020.10.075

Yin, P., Kong, X., Yue, Z., Yu, H., Li, Y., Li, J. (2023) Evaporation temperature prediction of a direct-expansion solar-assisted heat pump, *Solar Energy* 256, 215–224. https://doi.org/10.1016/j.solener.2023.03.052.

Zanetti, E., Azzolin, M., Girotto, S., Del Col, D. (2023) Performance and control of a CO2 dual source solar assisted heat pump with a photovoltaic-thermal evaporator, *Applied Thermal Engineering* 218, 119286. https://doi.org/10.1016/j.applthermaleng.2022.119286.

Zhang, D., Wu, Q. B., Li, J. P., Kong, X. (2014) Effects of refrigerant charge and structural parameters on the performance of a direct-expansion solar-assisted heat pump system. *Applied Thermal Engineering*. 73(1), 522-8. http://dx.doi.org/10.1016/j.applthermaleng.2014.07.077.